Determination of Diffusion Characteristics Using Two- and Four-Point Probe Measurements

Roger Brennan David Dickey
Solecon Laboratories, Inc., San Jose, California

By the use of two- and four-point probe measurements, much can be learned about the characteristics of a doped silicon wafer. The two-point probe system (spreading resistance probe) will provide resistivity *vs* depth profiles while the four-point probe system will indicate the uniformity of the diffusion over the surface of the wafer. Both systems have the same equation as their basis. The development of each system from this equation is discussed. Applications and the strengths and weaknesses of each system are discussed.

Solid state diffusion is a mechanism which dominates semiconductor fabrication processes. It permits the process engineer, within stringent limitations, to put dopants where they are wanted. Controlling diffusion is also essential to prevent doping where it is not wanted. Control requires measurement. Two methods of measuring dopant distribution resulting from solid state diffusion in silicon are discussed: spreading resistance analysis (SRA) and four-point probe analysis. Both methods are indirect in that they deal with electrical resistivity of the silicon rather than with actual counting of atoms. Fortunately, there is an intimate relationship between resistivity and dopant concentration in a semiconductor:

$$\rho = \left(Ne\mu\right)^{-1} \qquad (1)$$

where:

ρ = resistivity in ohm-cm
N = net dopant concentration in atoms/cm^3
e = electronic charge in coulombs
μ = majority carrier mobility in cm^2/volt-sec

Measuring electrical resistivity is therefore a viable way of determining dopant concentrations. The two measurement methods discussed here, used in concert, can provide a surprisingly complete characterization of a diffusion step or combination of steps. The spreading resistance probe has high spatial resolution and can detect variations in dopant concentration over very small distances. The four-point probe is relatively much more accurate and precise but samples a much larger volume of material; it can detect subtle variations in average concentrations over large distances. Both systems require the introduction of a test current into the specimen – and measurement of either a resulting voltage or a resistance. By solving the appropriate boundary value problem in potential theory, one can extract values of resistivity from just such simple measurements. The general approach and some of the mathematics for obtaining the resistivity are described in the Appendix.

Two-Point Probe System (Spreading Resistance Analysis)

Two probe tips, usually made of osmium and/or tungsten carbide, are employed. Each one is mounted on the end of a separate arm. Each arm pivots on a kinematic bearing system that virtually eliminates lateral motion of the probe tip as it contacts the sample surface. The probe tips are shaped such that they can be positioned very close together, often with less than a 20 μm separation (sometimes much less). The probe tips are lowered onto the sample as gently as possible. Because of the small contact area of the probe tip the pressure is quite high, in excess of a million pounds per square inch. The probe tip material is harder than the silicon and consequently fractures the silicon leaving “probe marks”.

Five millivolts are applied across the probes and the resistance (called spreading resistance) is measured. If the contact area of the probes is made small enough, the largest component of the measured resistance arises from the current crowding in the immediate vicinity of the probe tip. In the limiting case the relationship becomes:

$$R_s = \frac{\rho}{2a} \qquad (2)$$

where:

R_s = the measured spreading resistance (ohms)
ρ = the local resistivity (ohm-cm)
a = the radius of the contact area of the probe (cm)

This expression is an oversimplification. In practice, bulk samples whose resistivity is well documented are measured and a is then calculated. Seldom, if ever, are

Solecon Laboratories, Inc. ● 770 Trademark Drive ● Reno NV 89521-5926 ● Tel. (775) 853-5900 ● Fax (775) 853-5998

the contact areas of the probes truly circular or the same size. When unconstrained, the resistivity is sensed in a sampling volume that approximates a hemisphere with radius a. If there is an appreciable resistivity gradient through the sampling volume, then corrections need to be made for this. Corrections also will be needed if the sampling volume is distorted due to the proximity of a p-n junction, an insulator, or a region of much higher conductivity such as a buried layer. Several data reduction procedures have been developed to address these needed corrections. Generally, the data reduction programs employ either the multilayer potential distribution approach pioneered by Schumann and Gardner[1] or the local slope approach of Dickey[2], or a combination of the two.

In practice, an extensive calibration is required because of deviations from the relationship shown in equation 2. Solecon Labs uses 64 pieces of silicon whose resistivity is well documented. The samples are divided into four groups: p<111>, p<100>, n<111>, and n<100>. Each group has 16 samples ranging from .001 ohm-cm to 400 ohm-cm. In the calibration curves shown in figure 1, note the departures from the straight line relationship of equation 2. n-type material of a given resistivity produces higher spreading resistance readings than does p-type. n<111> material of a given resistivity produces higher spreading resistance readings than does n<100>. At low resistivities, the slope of the calibration curve changes rapidly and becomes flatter as the resistivity decreases. At the high end of the calibration curve, the slopes are relatively constant and estimates of resistivities much greater than 400 ohm-cm can be made.

Because the spreading resistance probe senses the resistivity in a microscopic sampling volume immediately under the probe tip, one can angle lap a silicon structure and then probe down the beveled surface obtaining a resistivity *vs* depth profile. A plot of carrier concentration *vs* depth can be calculated using published values of mobility[3]. Plots of carrier concentration *vs* depth are usually more convenient because they tend to follow the doping profile which the process engineer tries to control. The SRP does not sense doping type per se. As a separate operation, one of the probe tips can be heated and the polarity of the Seebeck voltage can be sensed to determine conductivity type.

Sample Preparation

Sample preparation is also an area of concern. Care must be used to avoid rounding the beveled edge, compromising the depth accuracy. Ideally, in the case of patterned samples, one should probe no closer to the diffusion mask edge than half the probe spacing. For the same reason, care should be taken not to bevel the sample closer than half the probe spacing to the edge of the diffusion mask (figure 2). Samples should be angle lapped (beveled) immediately prior to probing. Our experience has been that long waiting periods, such as overnight, tend to produce noisier data. The lapping method should be totally mechanical to minimize the introduction of non-stable surface charges[4]. The resultant bevel angle should be measured. Care must also be taken to minimize scratches on the beveled surface. Scratches change the probe contact area and thus compromise the calibration.

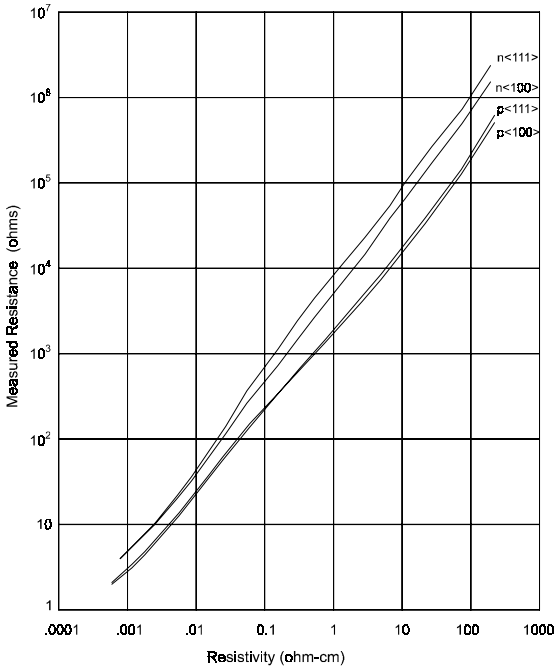

Figure 1. Calibration Chart of Spreading Resistance *vs* Resistivity

Probing

Spreading resistance measurements suffer from noise, *i.e.*: scatter in measured resistance on known homogenous material. Because the probes are lightly loaded and the contact area is very small, the way in which the probe tips contact the silicon varies. This causes variances in the measured resistance. The

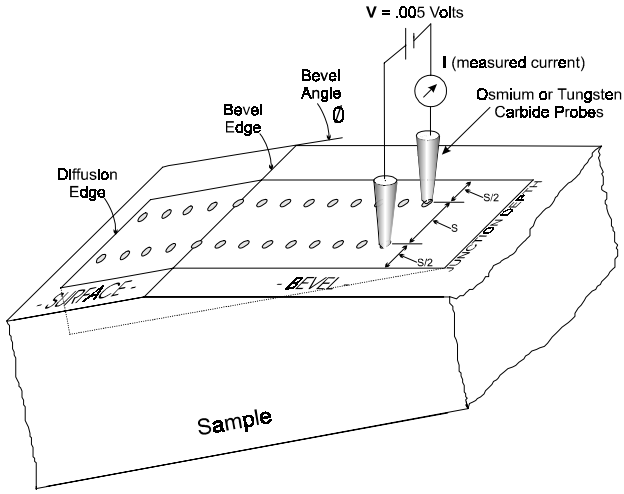

Figure 2. Illustration of a Spreading Resistance Measurement on a Beveled Sample

Solecon Laboratories, Inc. ● 770 Trademark Drive ● Reno NV 89521-5926 ● Tel. (775) 853-5900 ● Fax (775) 853-5998

noise can be reduced by increasing the load on the probe tip. This, however, increases the sampling volume and reduces the depth resolution. Typically, a probe tip loading of 2.5 grams is used for shallow structures X_j <0.5 µm and a loading of perhaps 10 grams for structures having junction depths one micron or deeper.

Care must also be taken to ensure that the probes travel in a path that is relatively free of scratches, perpendicular to the bevel edge, and that the step size is sufficient to prevent the probes from stepping into the previous probe marks. Preparation of probe tips is very much an art involving skill, patience, and trial and error. The desired properties of a well prepared pair of probe tips (some of which are diametrically opposed to each other) are low noise, small sampling volume, minimum penetration, close spacing, physical stability and compact size (no outlying contacts), and minimal damage to the silicon.

Data Reduction

Although the spreading resistance measurements are loaded directly into a computer containing the calibration data and the sampling volume correction algorithms, much human input is still required for the data reduction of each profile run, *e.g.*: bevel edge, start point, doping type(s), point(s) at which doping type changes, when to apply sampling volume correction, crystal orientation, step size, bevel angle measurement, adjustment for stray points and measurement of probe separation. In addition, the analyst must make judgement calls concerning problems that may arise with very shallow, very low dose surface layers due to geometrical effects and/or surface charges[5].

When differences in resistivity are relatively small (such as in the case of an ion implant threshold voltage adjustment on an MOS device), the relatively high noise of the spreading resistance measurement makes the data reduction uncertain. In many cases, C-V analysis may be better suited for this situation. The data reduction is also hampered at low resistivities due to the flatness of the calibration curve in this region. At concentrations above 1 X 10^{19} cm^{-3}, SIMS may be more accurate than SRA but the former senses atomic concentration whereas the latter senses carrier concentration and there may be large differences between them at low resistivities.

Examples

Base Diffusion:

The profile shown in figure 3 is for a base diffusion. A p-type dopant was introduced at the surface of an n-type substrate and then driven in. Note that the surface concentration is slightly less than the maximum which occurs at about 0.4 µm; not unusual when an oxidation is carried out concurrently with a boron base drive-in. The local resistivity was measured and the carrier concentration calculated from it. A junction depth of approximately 1.6 µm is indicated. The uncertainty of the depth scale for this and deeper structures is on the order of 3%. The uncertainty of carrier concentration values could be as much as 50% although much tighter values are usually seen. Often one can get a better idea of the accuracy by the following: The sheet resistivity of the p-layer can be calculated from the resistivity profile. One can then compare this calculated value with a more accurate method of determining sheet resistivity such as

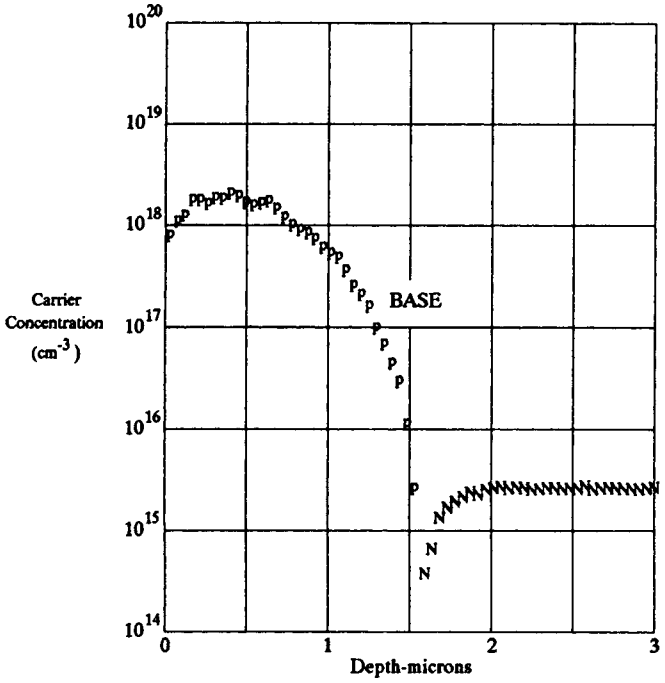

Figure 3. Base Diffusion

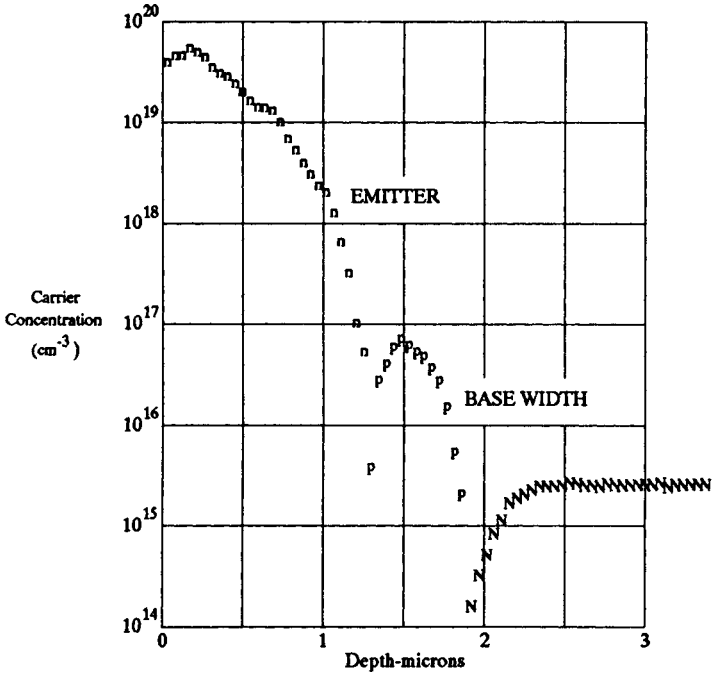

Figure 4. Emitter-Base Diffusion

Solecon Laboratories, Inc. ● 770 Trademark Drive ● Reno NV 89521-5926 ● Tel. (775) 853-5900 ● Fax (775) 853-5998

the use of a four-point probe, a Van der Pauw structure or perhaps a resistor of a known number of squares. This comparison often suggests whether the carrier concentrations (or resistivities) determined by the SRA are high or low. The dose in carriers/cm^2 can be calculated by summing the area under the p-curve and its accuracy can also be tested by the technique.

Enhanced Diffusion:

Figure 4 is a profile of the emitter base region on the same die as that used for the base profile shown above in figure 3. Note that the base junction depth is about 1.9 µm under the emitter in contrast to 1.6 µm in the area that did not have an emitter diffusion. This suggests the presence of the "emitter push effect"[6]. A little caution is suggested when comparing junction depths in different structures. The zero for depth is at the local silicon surface with no allowances made for topology. Offsets in the silicon surface due to the consumption of silicon by etching or oxidation must be considered. (In the present case, the emitter region suffered slightly greater silicon consumption than did the base because of the additional oxide removal step prior to emitter pre-deposition.)

Boron Contamination in Antimony:

The profile in figure 5 was taken immediately after epitaxial deposition. Note the slight dip between the epi and buried layer. Note also the anomalously high p-concentration below the buried layer. It is believed that the antimony used to dope the buried layer was contaminated with boron. During the buried layer drive-in, the boron outran the antimony and produced this p-tail. Then, during the epi deposition, the relatively small amount of diffusion associated with that operation caused sufficient boron to up-diffuse and compensate the epi region just above the buried layer. SRA is the only practical technique known by the authors which is capable of characterizing this situation.

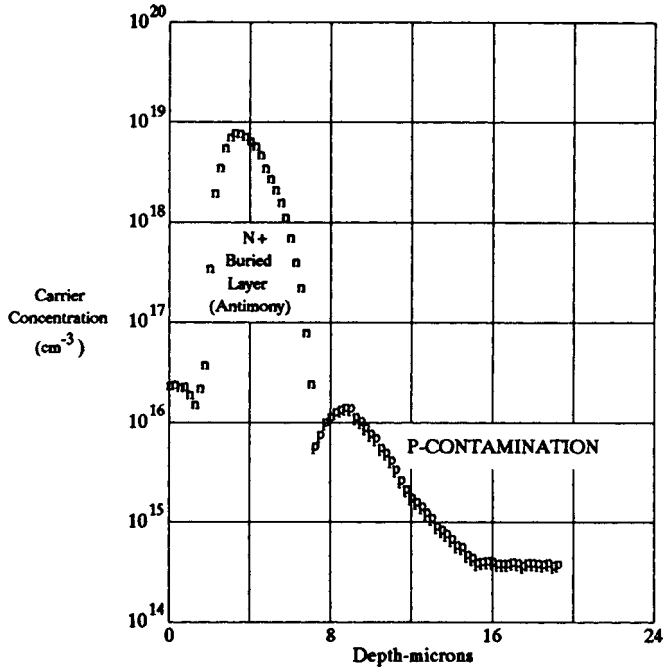

Figure 5. Boron Contaminated Antimony

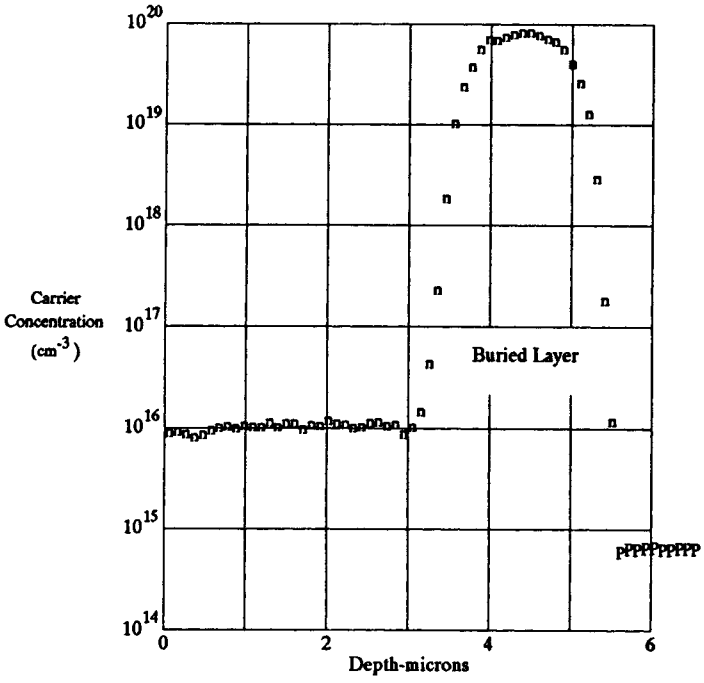

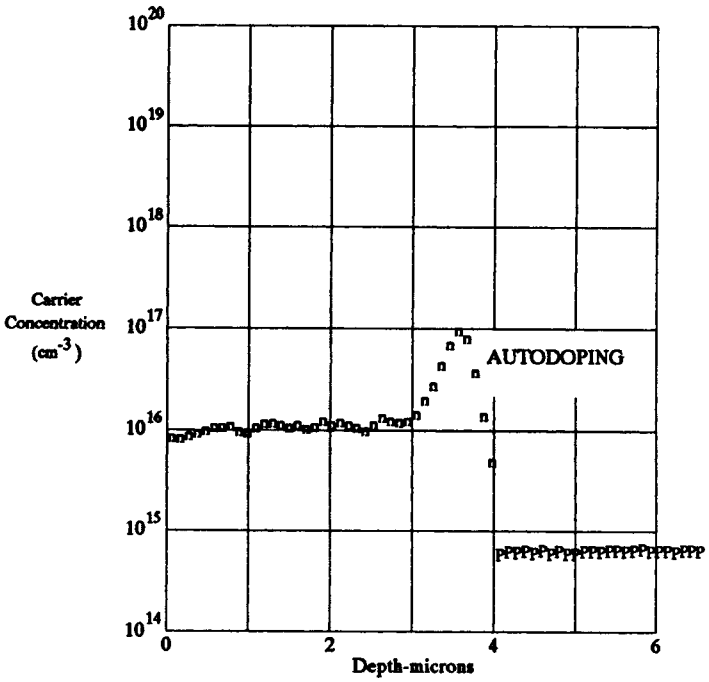

Figure 6. Arsenic Autodoping

Solecon Laboratories, Inc. ● 770 Trademark Drive ● Reno NV 89521-5926 ● Tel. (775) 853-5900 ● Fax (775) 853-5998

Arsenic Autodoping:

Arsenic and boron have sufficient vapor pressures at epitaxial deposition temperatures to produce significant autodoping during the start of epi growth[7]. Figure 6 shows two spreading resistance profiles, measured on the same bevel of a sample, immediately after an atmospheric pressure, $SiCl_4$ epi deposition. The first profile, taken through the buried layer pattern, indicates an epi thickness of about 3.5 µm with appreciable intrusion of the buried layer dopants up into the epi layer. Referring to the second profile, taken through the epi substrate, we see a ghost buried layer. The epi-thickness as indicated by the peak concentration is essentially the same 3.5 µm while the p-n junction is about 0.8 µm deeper and the peak concentration is roughly five times as great as the intentional epi concentration. This ghost buried layer would tend to cause the V/I on the epi test wafer to read deceptively low.

11 MeV Arsenic Implant:

Arsenic ions in the 5+ charge state were accelerated by a 2.2 megavolt terminal voltage to produce this impressive structure shown in figure 7. The implantation was done at the Lawrence Berkeley Lab[8].

Ion Implant Channeling:

Figure 8b shows a channeling "tail" which more than doubles the junction depth as compared with figure 8a. The shape of the profile in figure 8b is similar to that obtained by depositing and diffusing a slow and fast diffusing species (*e.g.*, antimony and phosphorus) concurrently. Frankly, we were surprised.

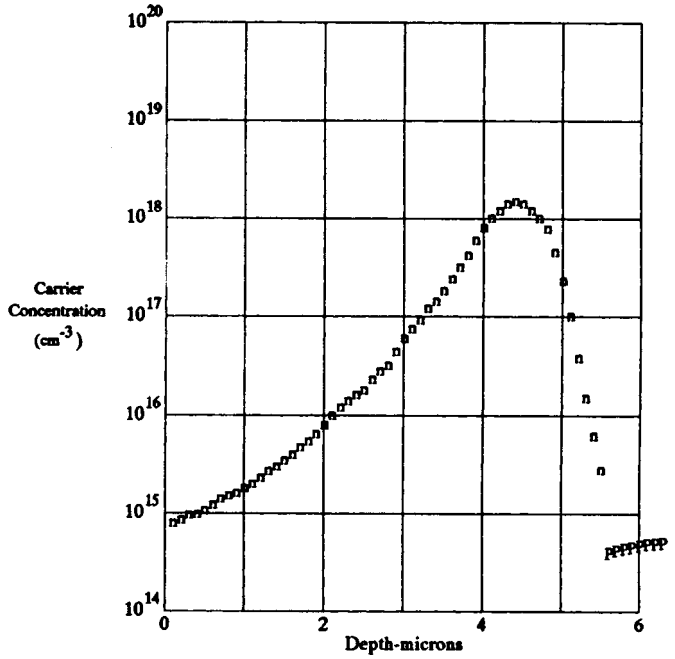

Figure 7. 11MeV Arsenic Implant

"Hydrogen" Effect:

Higher than expected surface resistivity has been observed on some p-type epi immediately after leaving the reactor. Figure 9b is the same sample after an air bake at only 200°C for 30 minutes. Pankove *et. al.*[9], have suggested "the hydrogenation of a silicon dangling bond at the site of a substitutional acceptor" (boron atom). Later, Chantre *et. al.*[10], reported similar observations on bulk p-type wafers.

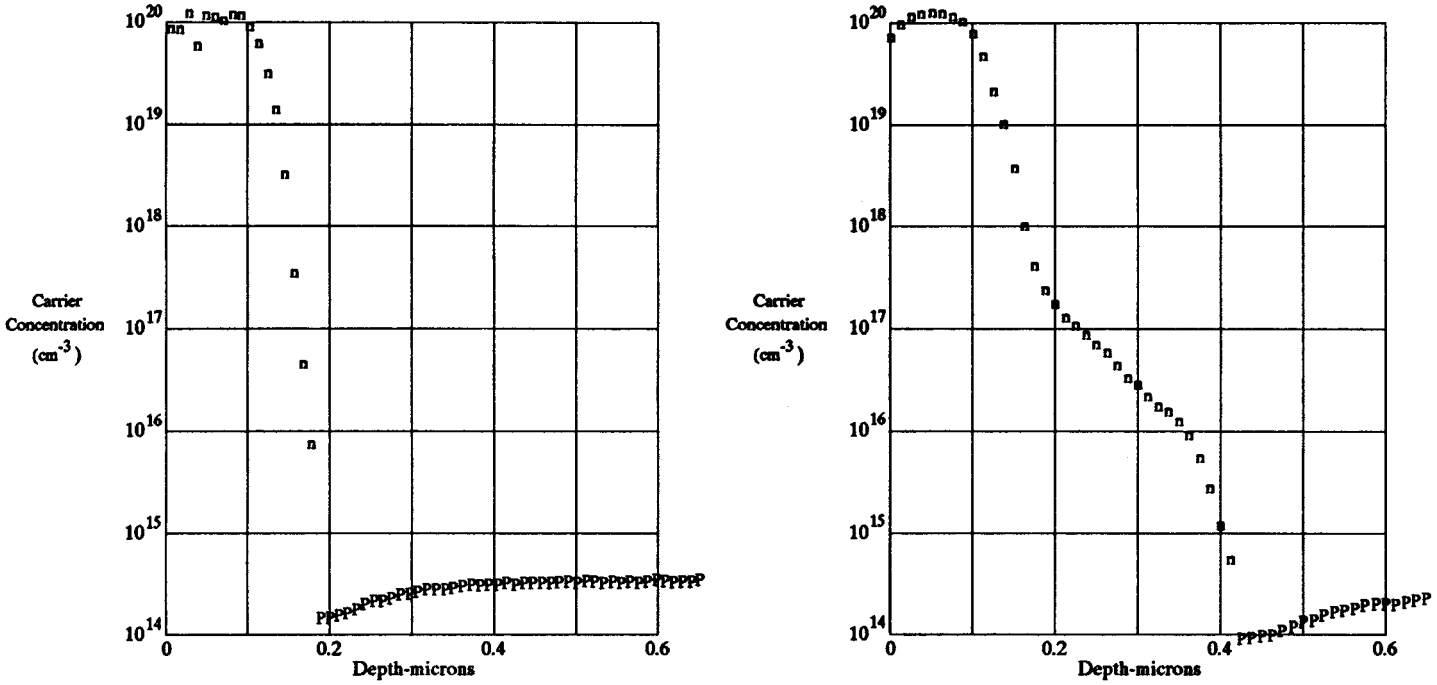

Figure 8. Ion Implant into <100> silicon. (a) 10° tilt, (b) 0° tilt

Solecon Laboratories, Inc. ● 770 Trademark Drive ● Reno NV 89521-5926 ● Tel. (775) 853-5900 ● Fax (775) 853-5998

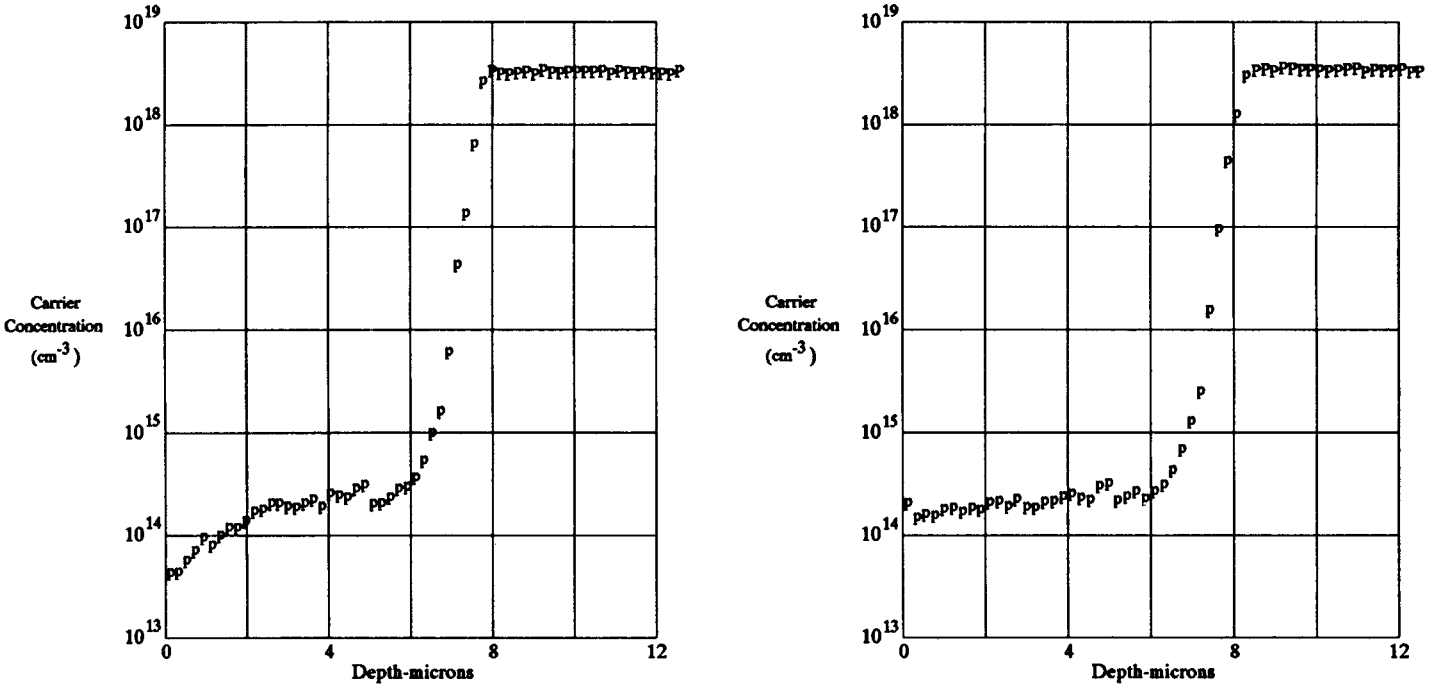

Figure 9. P-/P+ Epi. (a) profiled as received, (b) profiled after an air bake at 200°C

Epi /Substrate Interface:

The measured spreading resistances, an uncorrected resistivity profile and a resistivity profile corrected for sampling volume effects are shown in Figure 10. The uncorrected resistivities are obtained directly from the resistances by referring to the calibration curves. For this particular combination of probe conditioning and loading, a spreading resistance measurement of one ohm translates to roughly 0.0001 ohm-cm resistivity. All of the spreading resistance measurements within the epitaxial layer are influenced by the proximity of the junction, however, resulting in reduced sampling volume. Figure 10c shows the sampling-volume-corrected resistivities. The epi resistivity is seen to be almost constant, and its true value is significantly lower than the uncorrected value even at the surface. The epi/substrate interface is actually rather abrupt. (As is often the case, unfortunately, the corrected resistivities appear noisier.)

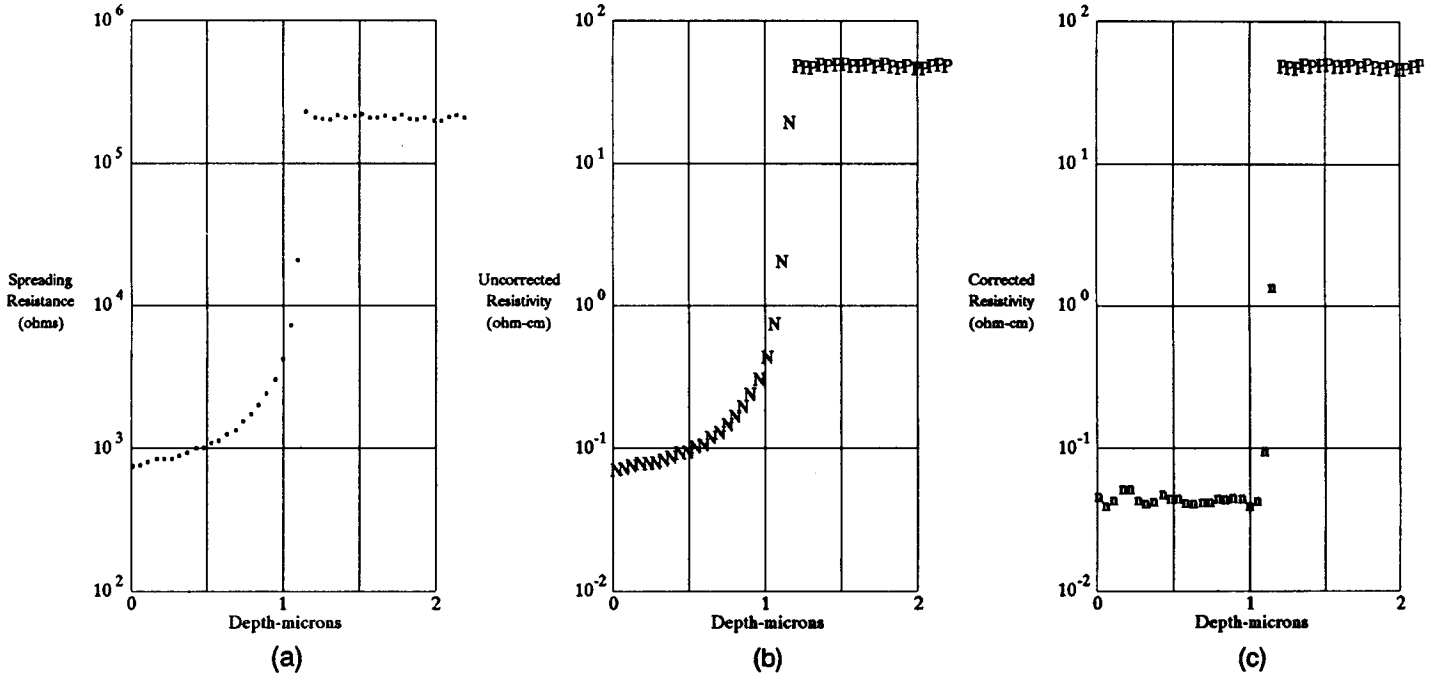

Figure 10. Thin N+ Epi on P- Substrate. (a) Measured Resistance, (b) Uncorrected Resistivity, (c) Corrected Resistivity

Solecon Laboratories, Inc. ● 770 Trademark Drive ● Reno NV 89521-5926 ● Tel. (775) 853-5900 ● Fax (775) 853-5998

Four-Point Probe System (Sheet Resistivity Contour Mapping)

When characterizing thin layers, it is useful to introduce the concept of resistance per unit area, or sheet resistivity. The sheet resistivity of a homogeneous layer is simply:

$$\rho_s = \frac{\rho}{t} \tag{3}$$

where t is the thickness of the layer. In most semiconductor applications, the carrier concentration, and therefore, the resistivity, will vary as a function of the depth, z, below the surface of the layer as shown in figure 11; *i.e.*:

$$\rho(z) = \left[\mathrm{N}(z) e \mu(N)\right]^{-1} \tag{4}$$

where N(z) is the carrier concentration as a function of depth, and $\mu(N)$ is the carrier mobility as a function of carrier concentration. Thus the sheet resistivity that is measured will be a weighted average given by:

$$\rho_s = \left[\int_0^t \mathrm{N}(z) e \mu(N) dz\right]^{-1} \tag{5}$$

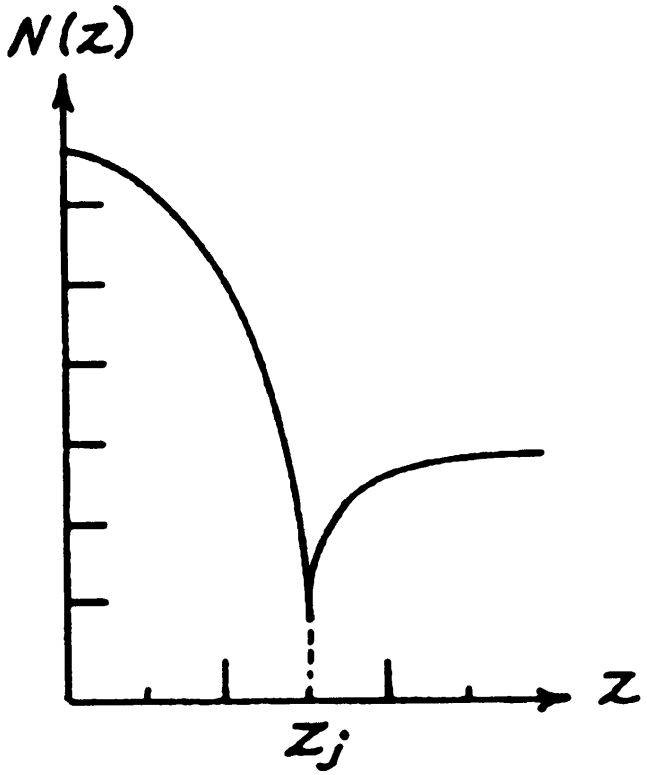

Figure 11. Variation of Carrier Concentration as a Function of Depth

where the integration is performed over the full thickness of the sample. For the case of a p-n junction isolated layer, the thickness t is equal to the junction depth z_j.

Four probe tips are arranged in a linear array as shown in figure 12. Probe force, probe travel, tip radius and probe material must be selected with consideration for the resistivity, hardness, and thickness of the layer to be measured. It is customary to have the outer two probes carry current and the inner probes measure the resultant voltage. If the probe spacings are equal ($S1 = S2 = S3$), then:

$$\rho_s = \left(\frac{\pi}{\ln 2}\right) R_a = 4.532 R_a \tag{6}$$

where $R_a = V_a/I$ and represents the average of the two resistance values obtained by reversing the polarity of the current supply. This procedure eliminates any voltage offsets in the circuit.

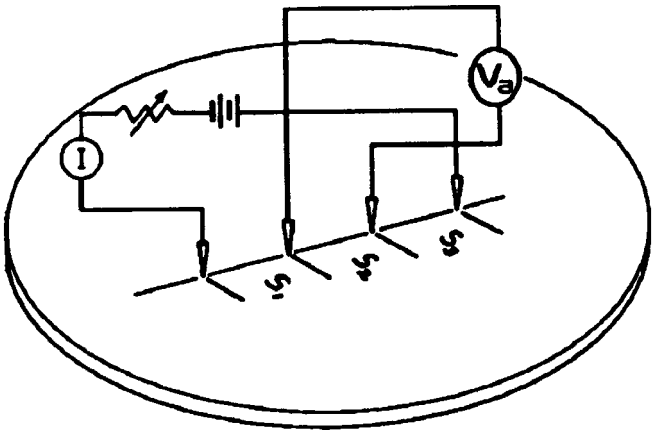

Figure 12. Linear Four-Point Probe Array; Conventional Configuration

In practice, the accuracy and repeatability of the measurements suffer from geometric effects caused by slight variations in the probe spacings and the influence of nonconducting wafer boundaries. Indeed, the probe spacings vary slightly each time the probe array contacts the wafer. Fortunately, there exists a self-compensation technique for eliminating geometric sources of error. Ideally, the four probes should be parallel to the radius of a circular wafer as indicated in figure 13; (β=0). However, the technique is still valid even if the probe array is perpendicular (β=90°) to the radius as long as $r\text{-}r_0 > 5S$, where S is the average probe spacing. In this technique, two paired resistances are measured subsequent to the contacting of the sample by the probe needles. The first, R_a, is obtained in the conventional manner; the outer probes carry current, whereas the inner probes measure the resulting voltage drop (figure 12). The second value, R_b, is obtained by having the first and third probes carry the current and the second

Solecon Laboratories, Inc. ● 770 Trademark Drive ● Reno NV 89521-5926 ● Tel. (775) 853-5900 ● Fax (775) 853-5998

and fourth probes measure voltage (figure 14). Then the sheet resistivity is given by:

$$\rho_s = k(\xi)R_a \qquad (7)$$

where $k(\xi)$, the geometrical correction factor, depends only on the ratio $\xi=R_a/R_b$

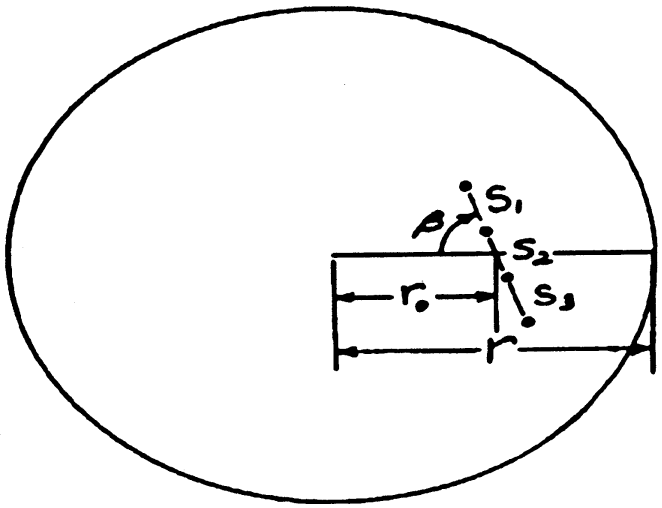

Figure 13. Geometric Influences for the Case of a Linear Four-Point Probe on a Circular Wafer

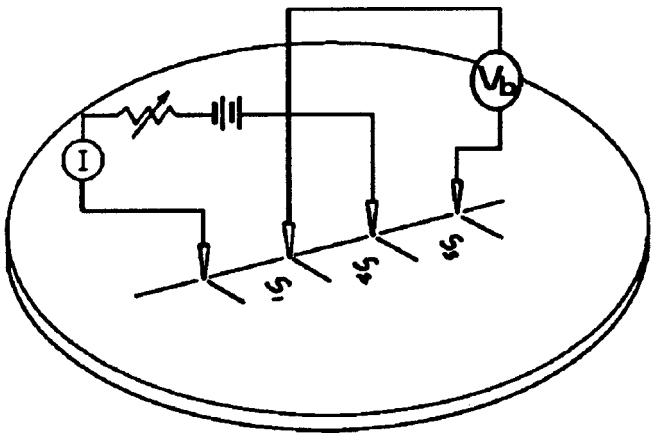

Figure 14. Linear Four-Point Probe Array; Second Measurement Configuration

Using paired-resistance measurements, one can achieve measurement accuracy of about ±0.5% and one sigma repeatability of 0.1% to 0.2%. With this degree of repeatability possible, sheet resistivity contour maps along with mean and standard deviation values can be produced, giving a rather clear picture of the uniformity of the top conductive layer. In practice, the primary use of the map is to characterize the uniformity of a given chemical/equipment system. While any number of "pre-deposition systems" (such as furnaces and jungle systems with gases, liquids, powdered solids, and solid discs, spin on dopants, spray on dopants, doped CVD glass, and ion implanters) can be forced to produce the

Figure 15. Four-Point Probe Contour Map After a Furnace Phosphorus Pre-Deposition

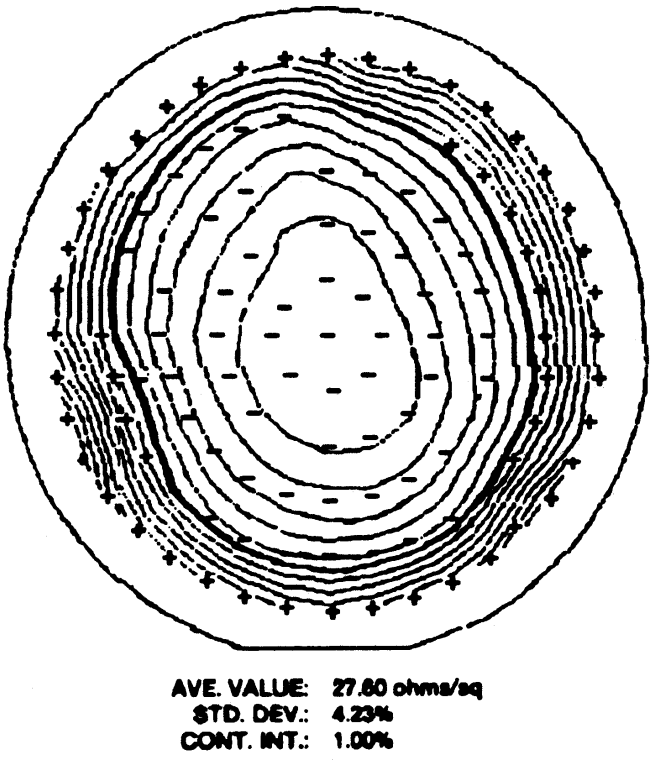

Figure 16. Four-Point Probe Contour Map After an Apparently Incomplete Anneal of an Ion Implant

same sheet rho at the center of the wafer, uniformity is an entirely different matter. A classic phosphorus pre-deposition is shown in figure 15. Note the resistivity is lowest at the edge and becomes increasingly higher towards the center, suggesting that the edge of the

wafer gets more doping than the center. Contrast that with figure 16 showing an ion implant after an apparently incomplete rapid anneal. Here, the center of the wafer has a lower sheet resistivity than that of the edge, probably due to the slower cooling of the center.

The setting up of any new process is not complete until uniformity is checked. Figure 17 is the contour map of a test wafer in a ladder boat. While the overall uniformity is impressive, one observes contour patterns probably due to the gas flow pattern in the tube.

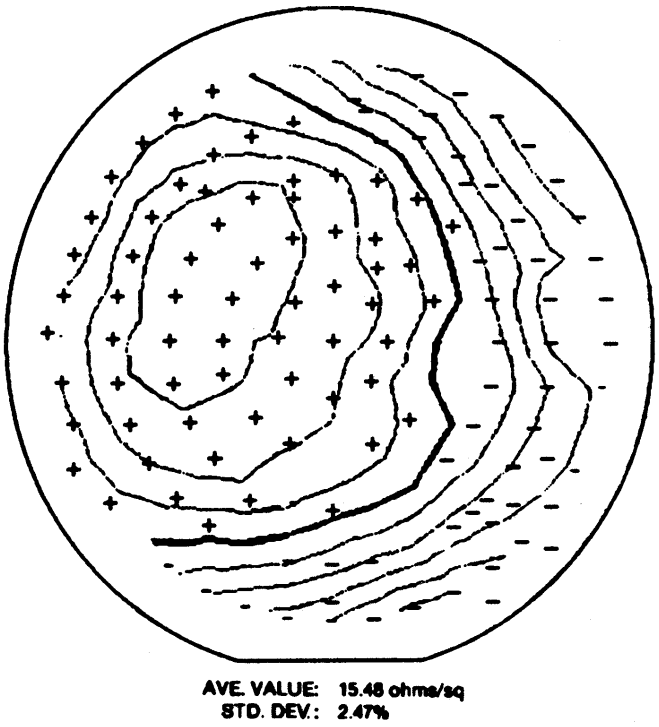

Figure 17. Four-Point Probe Contour Map After a Ladder Boat Pre-Deposition

Summary:

The two-point probe system (Spreading Resistance Analysis) provides general purpose and relatively inexpensive depth profiling with high spatial resolution and excellent depth accuracy. The procedure, which is destructive and highly technique dependent, has relatively high measurement noise and as a consequence, has substantial uncertainty in resistivity measurements. SRA has unmatched sensitivity at low doping levels but C-V analysis may be more accurate for channel regions in MOS devices and SIMS may be more accurate for concentrations >1x10^{19} cm^{-3}. In addition, problems have been noted with very shallow, very low dose surface layers due to geometrical effects and/or surface charges. Equipment maintenance and calibration are relatively involved.

The four-point probe system provides sheet resistivity contour maps of the top layer on a wafer with excellent accuracy and repeatability. Spatial resolution is not nearly as high as with SRA. Equipment maintenance and calibration are relatively easy. Generally speaking, SRA characterizes semiconductor processes and four-point probe contour mapping characterizes semiconductor processing equipment. The two techniques in concert provide the diffusion engineer a wealth of information.

Acknowledgments

The authors would like to thank Carlos DeMarchena, Monolithic Memories, Santa Clara, California, for the example of a ladder boat pre-deposition and Dave Perloff, Prometrix, Santa Clara, California, for four-point probe discussions.

Appendix

Notes on the Potential Distribution Equation:

A number of assumptions must be made in order to get even an approximate solution for the potential distribution around a contact carrying current into a sample having a known resistivity distribution. Among these assumptions are:

1. The contact is considered a flat disc with constant radius.
2. The resistivity varies in only one dimension, *viz.*, in depth below the surface.
3. Charge accumulation at boundaries is insignificant, permitting the use of LaPlace's equation rather than Poisson's equation.
4. The distribution of current over the area of the contact disc is known.

Under these assumptions, one can solve for the potential at any point on the surface of the specimen[1]:

$$V(r) = \frac{I\rho}{2\pi a}\int_0^\infty \left\{\left[1+2\theta(\lambda)\right]J_o(\lambda r)\frac{\sin(\lambda a)}{\lambda}\right\}d\lambda \qquad (8)$$

where r is the distance from the center of the current carrying disc contact, ρ is the resistivity at the surface, a is the radius of the contact, $\theta(\lambda)$ is a structure factor which contains all the information about how resistivity varies below the surface, and J_o is a Bessel function. This equation applies equally well to a spreading resistance measurement or a four-point probe measurement.

For spreading resistance measurement with probes arranged as shown in figure 18, we need to average the potential given by equation 8 over the surface of each contact. This leaves us with an integral equation similar to equation 8, which must be evaluated to obtain the potential difference between the two probes.

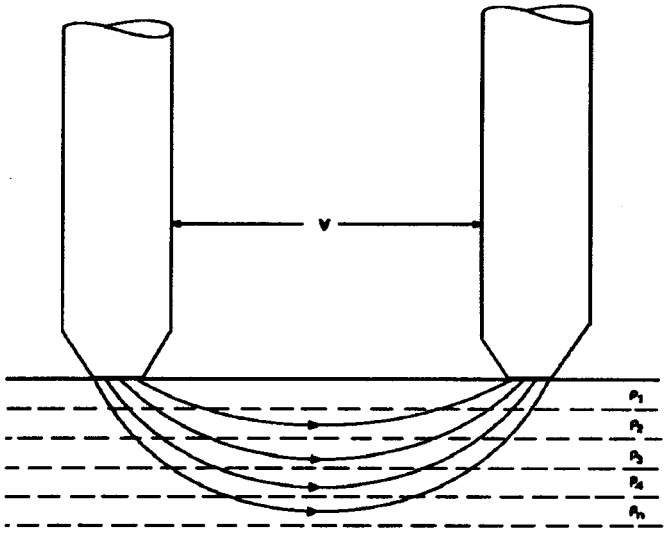

Figure 18. Spreading Resistance on a Multi-Layer Structure

With profile measurement (on a bevel), the structure factor $\theta(\lambda)$ can be determined to within a single constant related to the resistivity at the local surface. With all other parameters known, the integral can be evaluated for various estimates of surface resistivity until the calculated potential agrees with the actual applied potential. The boundary value problem is thus solved for that particular measurement point and one can use the result to determine the structure factor for the next point nearer the original surface. This procedure takes a substantial amount of computation time, but very efficient algorithms have been developed so that it is now common to do the analysis routinely with a dedicated microcomputer.

For a four-point probe arrangement as shown in figure 12, the potential difference between probes 2 and 3 is wanted. In principle, it is given in reference to equation 8 as:

$$V_2 - V_3 = 2V(s) - 2V(2s) \qquad (9)$$

In practice, though, we have no information about the structure factor since the four-point probe is used only at the original surface of the sample. Rather than trying to evaluate equation 8, the common procedure is to use the four-point probe to determine the sheet resistivity of the surface resistivity. For this purpose, the mathematics are much simpler, and the working equation is easily found[11]:

$$V_2 - V_3 = \frac{\ln 2}{\pi} I\rho_s \qquad (10)$$

References:

[1]Schumann and Gardner, J. Electrochem Society, vol. 116, pp.87-91 (1969).

[2]Dickey and Ehrstein, N.B.S. Special Publication 400-48, May 1979.

[3]Thurber, Mattis, Lin, and Filliben, N.B.S. Special Publication 400-64, May 1981, Table 10, p. 34 and Table 14, p. 40.

[4]Jim Ehrstein (private communication), National Bureau of Standards, Gaithersburg, MD 20899.

[5]S.M. Hu, J. Appl. Phys., vol. 53, pp. 1499-1510, March 1982.

[6]A.S. Grove, "Physics and Technology of Semiconductor Devices", p. 63, Wiley, New York. 1967.

[7]"VLSI Technology", S.M. Sze, ed., pp. 56-60, McGraw-Hill, New York, 1983.

[8]Peter Byme et. al. "Megavolt Arsenic implantation into Silicon", 1982 international Conference on Metallurgical Coating and Process Technology.

[9]J. I. Pankove et. al., Physical Review Letters, vol. 51 p. 2224., Dec. 12, 1983.

[10]Chantre et. al. J. Electrochemical Society, vol. 135, p. 2867-2868 (1988).

[11]L.B. Valdez Proc. IRE, vol. 42, p. 420 (1954).

Roger Brennan received his BS in Chemistry from Marshall University, Huntington, W. Va. in 1963. After working as a chemist for two years, he joined the Texas Instruments MOS development program in Dallas. For the next twelve years he worked in the area of masking and diffusion for a variety of companies as a process engineer. For the past nine years he has been the Laboratory Manager of Solecon's San Jose Lab, specializing in spreading resistance analysis. He is a part-time instructor in Semiconductor Processing at Foothill College, a member of the Greater Silicon Valley Implant Users' Group, and recording secretary of the local Electrochemical Society division.

David Dickey studied Engineering Physics at Montana State University, and received his BS degree in 1957. He worked at Westinghouse in Pittsburgh for several years, and was engaged in using measurement of spreading resistance to calculate doping profiles in silicon. He spent two years with Harshaw Chemical and then returned to Montana State for graduate studies in Physics. After receiving his Ph.D. in 1969, he worked for five years on research in magnetic materials. In 1975, Dr. Dickey founded Solecon Laboratories and has since served as its Director.